Turkish Journal of Mathematics

http://journals.tubitak.gov.tr/math/

Research Article

Turk J Math
(2018) 42: 373 – 394

doi:10.3906/mat-1609-69

An effective application of differential quadrature method based on modified cubic B-splines to numerical solutions of the KdV equation

Ali BAŞHAN*
Department of Mathematics, Faculty of Science and Arts, Bülent Ecevit University, Zonguldak, Turkey

Received: 23.09.2016 • **Accepted/Published Online:** 01.04.2017 • **Final Version:** 22.01.2018

Abstract: In this study, numerical solutions of the third-order nonlinear Korteweg–de Vries (KdV) equation are obtained via differential quadrature method based on modified cubic B-splines. Five different problems are solved. To show the accuracy of the proposed method, L_2 and L_∞ error norms of the problem, which has an analytical solution, and three lowest invariants are calculated and reported. The obtained solutions are compared with some earlier works. Stability analysis of the present method is also given.

Key words: KdV equation, differential quadrature method, modified cubic B-splines, partial differential equation, stability

1. Introduction

The present manuscript examines the KdV equation, described as

$$U_t + \varepsilon U U_x + \mu U_{xxx} = 0, \tag{1}$$

where subscripts t and x denote partial derivatives with respect to time and space, respectively, and ε and μ are constant parameters.

In the natural world, the Korteweg–de Vries (KdV) equation has been widely used to model a variety of nonlinear phenomena such as ion acoustic waves in plasmas, and shallow water waves. In the equation, the derivative U_t characterizes the time evolution of the wave propagating in one direction, the nonlinear term UU_x describes the steepening of the wave, and the linear term U_{xxx} stands for the spreading or dispersion of the wave. The KdV equation was derived by Korteweg and de Vries to describe shallow water waves of long wavelength and small amplitude. The KdV equation is a nonlinear evolution equation modeling a diversity of important finite amplitude dispersive wave phenomena. The equation has been the simplest nonlinear equation describing two important effects: nonlinearity, which is represented by UU_x, and linear dispersion, which is represented by U_{xxx}. Nonlinearity of UU_x tends to localize the wave whereas dispersion spreads the wave out. The stability of solitons is a result of the delicate equilibrium between the two effects of nonlinearity and dispersion [1, 2, 13, 17].

The differential quadrature method (DQM) was first introduced by Bellman et al.[9] in 1972. The DQM has widely become a preferable method in recent years due to its simplicity for application. Numerous researchers have developed different types of DQMs by utilizing various test functions such as Legendre polynomials and

*Correspondence: alibashan@gmail.com
2010 *AMS Mathematics Subject Classification:* 65D07, 65L20, 65M99, 65L06

spline functions [9, 10], Lagrange interpolation polynomials [23, 29, 30], Hermite polynomials [14], radial basis functions [32], harmonic functions [37], Sinc functions [12, 24], and B-spline functions [5–8, 20, 25, 26].

In the present manuscript, the modified cubic B-spline differential quadrature method (MCBC-DQM) is applied to obtain approximate solutions of the KdV equation. Since modified cubic B-splines are third-order functions, to obtain directly third-order weighting coefficients is impossible. To overcome this obstacle we used the matrix multiplication approach.

2. Modified cubic B-spline DQM

We are going to consider Eq. (1) with the following boundary conditions:

$$U(a,\ t)\ =\ g_1\,(t)\,,\qquad U(b,\ t)\ =\ g_2\,(t)\,,\qquad t\ \geq\ 0, \tag{2}$$

and with the following initial condition:

$$U(x,\ 0)\ =\ f(x),\qquad a\ \leq\ x\ \leq\ b, \tag{3}$$

where $g_1\,(t)$ and $g_2\,(t)$ are constants. The DQM can be defined as an approximation to a derivative of a given function by using the linear summation of its values at specific discrete grid points over the solution domain of a problem. Let us take the grid distribution $a = x_1 < x_2 < \cdots < x_N = b$ of a finite interval $[a,\ b]$ into consideration. Provided that any given function $U\,(x)$ is smooth enough over the solution domain, its derivatives with respect to x at a grid point x_i can be approximated by a linear summation of all the functional values in the solution domain, namely,

$$U_x^{(r)}\,(x_i)\ =\ \frac{d^{(r)}U}{dx^{(r)}}\,|_{x_i}\ =\ \sum_{j=1}^{N} w_{ij}^{(r)}U\,(x_j)\,,\quad i\ =\ 1,\ 2,\ ...,\ N,\quad r\ =\ 1,\ 2,\ ...,\ N-1, \tag{4}$$

where r denotes the order of derivative, $w_{ij}^{(r)}$ represents the weighting coefficients of the $r-th$ order derivative approximation, and N denotes the number of grid points in the solution domain. Here the index j represents the fact that $w_{ij}^{(r)}$ is the corresponding weighting coefficient of the functional value $U\,(x_j)$.

In this study, we are going to need the first- and third-order derivatives of the function $U(x)$. However, third-order derivatives of the cubic B-spline functions do not exist. Hence, we are going to find the value of the equation (4) for the $r = 1$ and then by using first- and second-order weighting coefficients obtain third-order weighting coefficients.

If we consider Eq. (4) carefully, we see that the fundamental process for approximating the derivatives of any given function through the DQM is to find out the corresponding weighting coefficients $w_{ij}^{(r)}$. The main idea behind DQM approximation is to find out the corresponding weighting coefficients $w_{ij}^{(r)}$ by means of a set of base functions spanning the problem domain. While determining the corresponding weighting coefficients, a different basis may be used. In the present study, we are going to try to compute weighting coefficients with a modified cubic B-spline basis.

Let $Q_m(x)$ be the cubic B-splines with knots at the points x_i, where the uniformly distributed N grid points are taken as $a = x_1 < x_2 < \cdots < x_N = b$ on the ordinary real axis. Then the cubic B-splines $\{Q_0,$

$Q_1,\ \ldots,\ Q_{N+1}\}$ form a basis for functions defined over $[a,\ b]$. The cubic B-splines $Q_m(x)$ are defined by the relationships:

$$Q_m(x) = \frac{1}{h^3}\begin{cases}(x-x_{m-2})^3, & x\in[x_{m-2},\ x_{m-1}],\\ (x-x_{m-2})^3-4(x-x_{m-1})^3, & x\in[x_{m-1},\ x_m],\\ (x_{m+2}-x)^3-4(x_{m+1}-x)^3, & x\in[x_m,\ x_{m+1}],\\ (x_{m+2}-x)^3 & x\in[x_{m+1},\ x_{m+2}],\\ 0, & otherwise.\end{cases}$$

where $h = x_m - x_{m-1}$ for all m. [28] The values of cubic B-splines and its derivatives at the grid points are given in Table 1.

Table 1. The value of cubic B-splines and derivatives functions at the grid points.

x	x_{m-2}	x_{m-1}	x_m	x_{m+1}	x_{m+2}
Q_m	0	1	4	1	0
Q_m'	0	$\frac{3}{h}$	0	$\frac{-3}{h}$	0
Q_m''	0	$\frac{6}{h^2}$	$\frac{-12}{h^2}$	$\frac{6}{h^2}$	0

Using the modified cubic B-splines results in a diagonally dominant matrix system of equations. This structure has great importance for the stability analysis. Modification of cubic B-splines can be carried out differently. Among others, Mittal and Jain [27] have introduced modified cubic B-splines at the grid points as follows:

$$\begin{aligned}\phi_1(x) &= Q_1(x) + 2Q_0(x)\\ \phi_2(x) &= Q_2(x) - Q_0(x)\\ \phi_k(x) &= Q_k(x) \text{ for } k = 3,\ 4,\ ...,\ N-2\\ \phi_{N-1}(x) &= Q_{N-1}(x) - Q_{N+1}(x)\\ \phi_N(x) &= Q_N(x) + 2Q_{N+1}(x),\end{aligned} \tag{5}$$

where ϕ_k, $(k = 1,\ 2,\ ...,\ N)$ forms a basis functions over the $[a,\ b]$ domain. This modification provides some advantages such as having a larger stability region and does not need any additional equations to obtain weighting coefficients like the cubic-DQM [22].

2.1. Weighting coefficients of first-order derivatives

From Eq. (4) with value of $r = 1$, we have obtained

$$\phi_k'(x_i) = \sum_{j=1}^{N} w_{i,j}^{(1)}\phi_k(x_j) \text{ for } i = 1,\ 2,\ ...,\ N;\ k = 1,\ 2,\ ...,\ N \tag{6}$$

equation. For the first grid point x_1 (6), we get the form

$$\phi_k'(x_1) = \sum_{j=1}^{N} w_{1,j}^{(1)}\phi_k(x_j) \text{ for } k = 1,\ 2,\ ...,\ N \tag{7}$$

and by using the value of modified cubic basis functions

$$\begin{bmatrix} 6 & 1 & & & & & \\ 0 & 4 & 1 & & & & \\ & 1 & 4 & 1 & & & \\ & & \ddots & \ddots & \ddots & & \\ & & & 1 & 4 & 1 & \\ & & & & 1 & 4 & 0 \\ & & & & & 1 & 6 \end{bmatrix} \begin{bmatrix} w_{1,1}^{(1)} \\ w_{1,2}^{(1)} \\ w_{1,3}^{(1)} \\ \vdots \\ \\ w_{1,N-1}^{(1)} \\ w_{1,N}^{(1)} \end{bmatrix} = \begin{bmatrix} -6/h \\ 6/h \\ 0 \\ \vdots \\ \\ 0 \\ 0 \end{bmatrix} \tag{8}$$

equation system is obtained. Similarly, by using the value of modified cubic basis functions at the x_i, $(2 \leq i \leq N-1)$ grid points, respectively,

$$\begin{bmatrix} 6 & 1 & & & & & \\ 0 & 4 & 1 & & & & \\ & 1 & 4 & 1 & & & \\ & & \ddots & \ddots & \ddots & & \\ & & & 1 & 4 & 1 & \\ & & & & 1 & 4 & 0 \\ & & & & & 1 & 6 \end{bmatrix} \begin{bmatrix} w_{i,1}^{(1)} \\ \vdots \\ w_{i,i-1}^{(1)} \\ w_{i,i}^{(1)} \\ w_{i,i+1}^{(1)} \\ \vdots \\ w_{i,N}^{(1)} \end{bmatrix} = \begin{bmatrix} 0 \\ \vdots \\ 0 \\ -3/h \\ 0 \\ 3/h \\ 0 \\ \vdots \\ 0 \end{bmatrix} \tag{9}$$

equation system is obtained. For the last grid point x_N

$$\begin{bmatrix} 6 & 1 & & & & & \\ 0 & 4 & 1 & & & & \\ & 1 & 4 & 1 & & & \\ & & \ddots & \ddots & \ddots & & \\ & & & 1 & 4 & 1 & \\ & & & & 1 & 4 & 0 \\ & & & & & 1 & 6 \end{bmatrix} \begin{bmatrix} w_{N,1}^{(1)} \\ w_{N,2}^{(1)} \\ \vdots \\ \\ w_{N,N-2}^{(1)} \\ w_{N,N-1}^{(1)} \\ w_{N,N}^{(1)} \end{bmatrix} = \begin{bmatrix} 0 \\ 0 \\ \vdots \\ \\ 0 \\ -6/h \\ 6/h \end{bmatrix} \tag{10}$$

equation system is obtained. Thus, weighting coefficients $w_{i,j}^{(1)}$, which are related to x_i, $(i = 1, 2, ..., N)$ are found quite easily by solving (8), (9), and (10) equation systems with the Thomas algorithm.

2.2. Weighting coefficients of second-order derivatives

This method depends on the first-order weighting coefficients when obtaining weighting coefficients of the second-order derivatives. By Shu's recurrence formula, the second-order weighting coefficients are determined for $i = 1, 2, ..., N$ and $j = 1, 2, ..., N$ as below [33]:

$$w_{i,j}^{(2)} = 2w_{i,j}^{(1)} \left(w_{i,i}^{(1)} - \frac{1}{(x_i - x_j)} \right), \qquad \text{for } i \neq j \tag{11}$$

$$w_{i,i}^{(2)} = -\sum_{j=1,\ j\neq i}^{N} w_{i,j}^{(2)} \tag{12}$$

2.3. Weighting coefficients of third-order derivatives

This method depends on the first- and second-order weighting coefficients to obtain weighting coefficients of the third-order derivatives. By the matrix multiplication approach, the third-order weighting coefficients are determined as below [33]:

$$\left[A^{(m)}\right] = \left[A^{(1)}\right]\left[A^{(m-1)}\right] = \left[A^{(m-1)}\right]\left[A^{(1)}\right], \qquad m = 2,\ 3,\ ...,\ N-1, \tag{13}$$

where $\left[A^{(m-1)}\right]$ and $\left[A^{(m)}\right]$ are the weighting coefficient matrices of the $(m-1)-th$ and $m-th$ order derivatives, respectively. Although equation (13) looks simple, it involves more arithmetic operations as compared to (11) and (12). It is noted that the calculation of each weighting coefficient by Eq. (13) involves N multiplications and $(N-1)$ additions, i.e. a total of $(2N-1)$ arithmetic operations. On the other hand, Shu's recurrence relationship (11) involves two multiplications, one division, and one subtraction, i.e. a total of four arithmetic operations [33].

3. Numerical discretization

The KdV equation of the form

$$U_t + \varepsilon U U_x + \mu U_{xxx} = 0, \tag{14}$$

with the boundary conditions (2) and the initial condition (3) is rewritten as

$$U_t = -\varepsilon U U_x - \mu U_{xxx} \tag{15}$$

Then the differential quadrature derivative approximations of the first and the third orders have been used in Eq. (15)

$$\frac{dU(x_i)}{dt} = -\varepsilon U(x_i,t)\sum_{j=1}^{N} w_{i,j}^{(1)} U(x_j,t) - \mu \sum_{j=1}^{N} w_{i,j}^{(3)} U(x_j,t), \qquad i = 1,\ 2,\ ...,\ N \tag{16}$$

and ordinary differential equation (16) is obtained. Then the ordinary differential equation given by (16) is integrated in time by means of an appropriate method. Here we have preferred the strong stability-preserving Runge–Kutta (SSP-RK43) method [36] due to its advantages such as accuracy, stability, and memory allocation properties. By using different types time integration methods and obtaining second- and third-order weighting coefficients by Shu's recurrence relationship and matrix multiplication approach the numerical results will change. Thus, we may say by using MCBC-DQM and SSP-RK43 together a hybrid method has been applied.

4. Numerical examples and stability

In this section, we have obtained the numerical solutions of the KdV equation by the MCBC-DQM. The accuracy of the numerical method is checked by using the error norms L_2 and L_∞, respectively:

$$L_2 = \left\|U^{exact} - U_N\right\|_2 \simeq \sqrt{h\sum_{J=1}^{N}\left|U_j^{exact} - (U_N)_j\right|^2},$$

$$L_\infty = \left\|U^{exact} - U_N\right\|_\infty \simeq \max_j\left|U_j^{exact} - (U_N)_j\right|,\ j = 1,\ 2,\ ...,\ N-1. \tag{17}$$

The following lowest three invariants corresponding to conservation of mass, momentum, and energy will be computed:

$$I_1 = \int_a^b U dx, \qquad I_2 = \int_a^b U^2 dx, \qquad I_3 = \int_a^b \left[U^3 - \frac{3\mu}{\varepsilon} \left(U' \right)^2 \right] dx. \tag{18}$$

Relative changes in invariants are defined as $\widehat{I_j} = \frac{I_j^{final} - I_j^{initial}}{I_j^{initial}},\ j = 1,\ 2,\ 3.$

Stability analysis of a numerical method for a nonlinear differential equation requires the determination of eigenvalues of coefficient matrices. With the numerical discretization of the partial differential equation KdV, it turns into an ordinary differential equation.

The stability of a time-dependent problem:

$$\frac{\partial U}{\partial t} = l(U), \tag{19}$$

with the proper initial and boundary conditions, where l is a spatial differential operator. After discretization with the DQM, Eq. (19) is reduced to a set of ordinary differential equations in time as follows:

$$\frac{d\{u\}}{dt} = [A]\{u\} + \{b\}, \tag{20}$$

where $\{u\}$ is an unknown vector of the functional values at the grid points except the left and right boundary points, $\{b\}$ is a vector containing the nonhomogeneous part and the boundary conditions and A is the coefficient matrix. The stability of a numerical scheme for numerical integration of Eq. (20) depends on the stability of the ordinary differential Eq. (20). If the ordinary differential Eq. (20) is not stable, numerical methods may not generate converged solutions. The stability of Eq. (20) is related to the eigenvalues of the matrix A, since its exact solution is directly determined by the eigenvalues of the matrix A. When all $Re(\lambda_i) \leq 0$ for all i it is enough to show the stability of the exact solution of $\{u\}$ as $t \to \infty$, where $Re(\lambda_i)$ denotes the real part of the eigenvalues λ_i of the matrix A. The matrix A in Eq. (20) is determined as $A_{ij} = -\varepsilon \alpha_i w_{i,j}^{(1)} - \mu w_{i,j}^{(3)}$, where $\alpha_i = U(x_i, t)$ [33]. The eigenvalues of matrix A should be in the stability region as shown in Figure 1 [21].

4.1. Single soliton

The initial condition:

$$U(x,\ 0) = 3C \sec h^2 (Ax + D), \tag{21}$$

where A, C, and D are constants given by the boundary conditions $U(0,\ t) = U(2,\ t) = 0$ for all times.

For this condition, the KdV equation has an analytic solution given in the form of

$$U(x,\ t) = 3C \sec h^2 (Ax - Bt + D), \tag{22}$$

provided that

$$A = \frac{1}{2} (\varepsilon C / \mu)^{1/2} \text{ and } B = \frac{1}{2} \varepsilon C (\varepsilon C / \mu)^{1/2}, \tag{23}$$

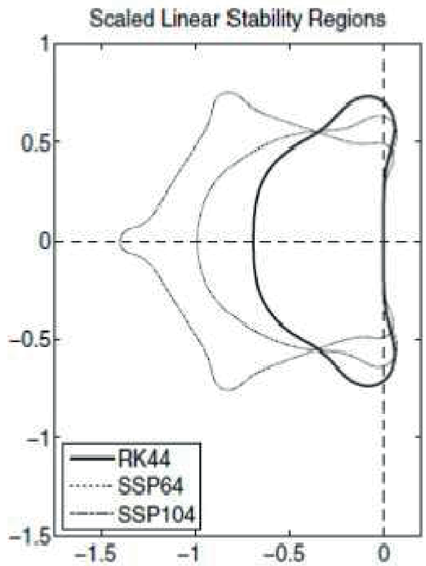

Figure 1. Stability regions of fourth order SSPRK eigenvalues.

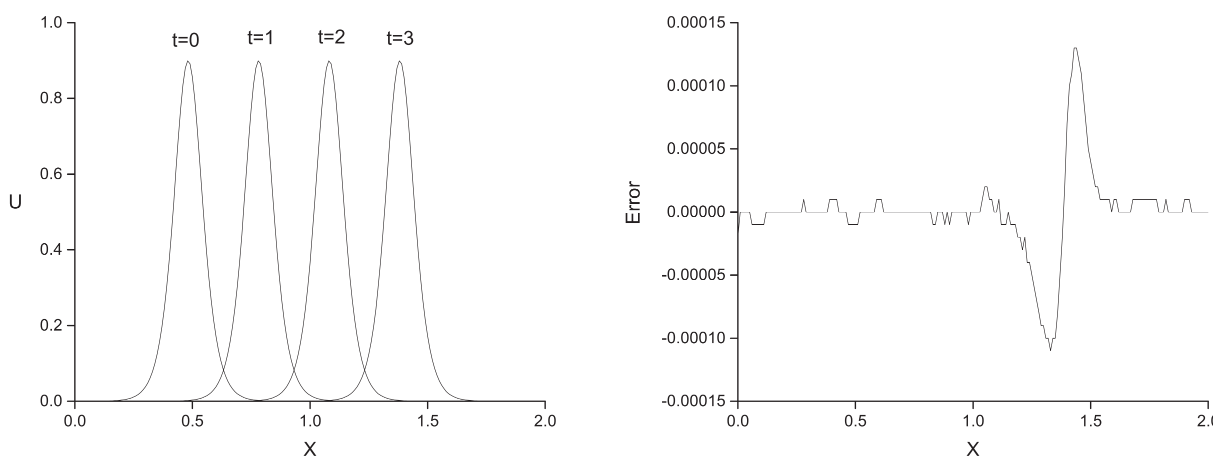

Figure 2. Single soliton solution for $\Delta t = 0.0005$ and $N = 201$ and error(U - U_N) at time t = 3.

so that (22) yields a probable initial condition when $A = \frac{1}{2}(\varepsilon/\mu)^{1/2}$ and really simulates a single soliton that moves toward the right having the velocity εC.

To be able to make a comparison with earlier studies, $\varepsilon = 1$, $\mu = 4.84 \times 10^{-4}$, $C = 0.3$, $D = -6$, $\Delta t = 0.0005$, and $N = 201$ will be used. For the present case, the obtained solution is going to move toward the right, having a speed of εC. Simulations of single soliton time up to $t = 3$ and the error value between analytical and numerical solutions are given in Figure 2. If we plot the graphs of the numerical solution and the exact solution, their curves will be indistinguishable. The agreement is very good. To make a comparison quantitatively, we have also computed the error norms L_2 and L_∞ in Table 2 and Table 3. Moreover, the first three invariants I_1, I_2, and I_3 and relative changes in invariants are reported in Table 4 until $t = 3$.

In Table 2, the L_2 norm is less than 4.7×10^{-5} while the L_∞ norm is less than 1.3×10^{-4} at time $t = 3$ and so they are small enough to be accepted. As it is straightforwardly seen from Table 2, the present

Table 2. Comparison of L_2 and L_∞ error norms at various times.

$L_2 \times 10^6$ error norms at various times	ε	$\mu \times 10^4$	N	Δt	Time		
					1	2	3
MCBC-DQM (Present)	1	4.84	101	0.001	348.3	658.2	972.7
	1	4.84	160	0.001	47.6	91.3	134.7
	1	4.84	201	0.0005	17.5	31.2	46.0
Zabusky [39]	1	4.84	200	0.0005	28660.0		
Galerkin [3]	1	4.84	200	0.0005	18720.0		
Septic spline Coll.[34]	1	4.84	200	0.005	22100.0		
Petrov-Galerkin [31]	1	4.84	200	0.005	13260.0		
Mod. Petrov-Galerkin [31]	1	4.84	200	0.005	740.0		
RBF Coll TPS [15]	1	4.84	200	0.005	4338.1		2606.0
RBF Coll IMQ [15]	1	4.84	200	0.005	2210.4		2751.0
RBF Coll IQ [15]	1	4.84	200	0.005	754.1		1013.0
RBF Coll MQ [15]	1	4.84	200	0.005	26.0		62.0
RBF Coll G [15]	1	4.84	200	0.005	26.7		46.0
Galerkin quad-spline [18]	1	4.84	200	0.005	60.0	86.0	107.0
Galerkin cubic-spline [19]	1	4.84	200	0.005	90.0	180.0	280.0
Subdomain [35]	1	4.84	200	0.001	22200.0		
LPDQ [23]	1	4.84	100	0.001	1185.0	1290.0	1381.0
QBDQM [6]	1	4.84	101	0.001	227.1	354.5	485.2
$L_\infty \times 10^5$ error norms at various times	ε	$\mu \times 10^4$	N	Δt	Time		
					1	2	3
MCBC-DQM (Present)	1	4.84	101	0.001	106.9	187.7	268.0
	1	4.84	160	0.001	14.2	26.7	38.2
	1	4.84	201	0.0005	5.4	9.2	12.9
Zabusky [39]	1	4.84	200	0.0005	813.0		
Galerkin [3]	1	4.84	200	0.0005	491.0		
RBF Coll TPS [15]	1	4.84	200	0.005			634.5
RBF Coll IMQ [15]	1	4.84	200	0.005			501.8
RBF Coll IQ [15]	1	4.84	200	0.005			209.0
RBF Coll MQ [15]	1	4.84	200	0.005			13.3
RBF Coll G [15]	1	4.84	200	0.005			13.6
Petrov-Galerkin [31]	1	4.84	200	0.005	383.0		
Mod. Petrov-Galerkin [31]	1	4.84	200	0.005	21.0		
LPDQ [23]	1	4.84	100	0.001	274.5	224.0	242.2
QBDQM [6]	1	4.84	101	0.001	73.8	108.6	142.8
Local scheme [38]	6	10000	250	0.125	173.0		
Global scheme [38]	6	10000	308	0.12	477.0		

Table 3. Comparison of L_2 and L_∞ error norms at time t=3.0.

				MCBC-DQM (Present)		Cubic-DQM [22]		Quartic-DQM[22]	
ε	$\mu \times 10^4$	N	Δt	$L_2 \times 10^6$	$L_\infty \times 10^5$	$L_2 \times 10^6$	$L_\infty \times 10^5$	$L_2 \times 10^6$	$L_\infty \times 10^5$
1	4.84	81	10^{-6}	2698.1	771.3	4560	854	2600	704
1	4.84	101	10^{-6}	972.6	268.0	3320	544	1700	434
1	4.84	151	10^{-6}	187.6	53.1	2010	382	850	328
1	4.84	201	10^{-6}	45.8	12.8	-	-	-	-
1	4.84	301	10^{-6}	24.3	6.3	-	-	-	-

Table 4. Invariants for single soliton: $\Delta t = 0.0005$ and $N = 201$.

t	$I_1 \times 10^1$	$I_2 \times 10^2$	$I_3 \times 10^2$	$\widehat{I}_1$	$\widehat{I}_2$	$\widehat{I}_3$
0.0	1.44598000	8.67592500	4.68506900	-	-	-
1.0	1.44598000	8.67592400	4.68506800	0.0×10^{-9}	-1.1×10^{-7}	-2.1×10^{-7}
2.0	1.44597900	8.67592500	4.68506600	-6.9×10^{-7}	0.0×10^{-9}	-6.4×10^{-7}
3.0	1.44598100	8.67592600	4.68507000	6.9×10^{-7}	1.1×10^{-7}	2.1×10^{-7}

results are in good agreement with those given in earlier works. To show the difference between the cubic-DQM and MCBC-DQM a comparison of results with the same parameters is given in Table 3. It is obviously seen from Table 3 that the present results are better than those of the cubic-DQM [22]. As it is straightforwardly seen from Table 4, the absolute maximum relative changes of invariants are less than 7.0×10^{-7}, 1.2×10^{-7}, and 6.5×10^{-7}, respectively, during all simulations. We may say that the three invariants computed are satisfactorily constant.

4.2. Double solitons

Our second test problem has the initial condition given in [15]

$$U(x,0) = 3c_1 \sec h^2 (A_1 x + D_1) + 3c_2 \sec h^2 (A_2 x + D_2), \tag{24}$$

and boundary conditions

$$U(0,\ t) = U(2,\ t) = 0, \tag{25}$$

where $\varepsilon = 1$, $\mu = 4.84 \times 10^{-4}$, $C_1 = 0.3$, $C_2 = 0.1$, $D_1 = D_2 = -6$, $\Delta t = 0.0005$ and $N = 201$ will be considered in all simulations.

As seen noticeably in Figure 3 the greater soliton, which has 0.9 amplitude, is located at the left of the smaller soliton initially. By the time the faster soliton has caught the slower one and at the end of the simulation the double solitons have a reverse situation. The invariants I_1, I_2 and I_3 are recorded and reported with relative changes in invariants in Table 5 for the present case. It is noticeably seen from Table 8 that the maximum absolute values of relative changes in invariants are less than 2.6×10^{-5}, 5.6×10^{-6} and 2.1×10^{-5}, respectively, during the simulation and therefore they can be considered almost constant.

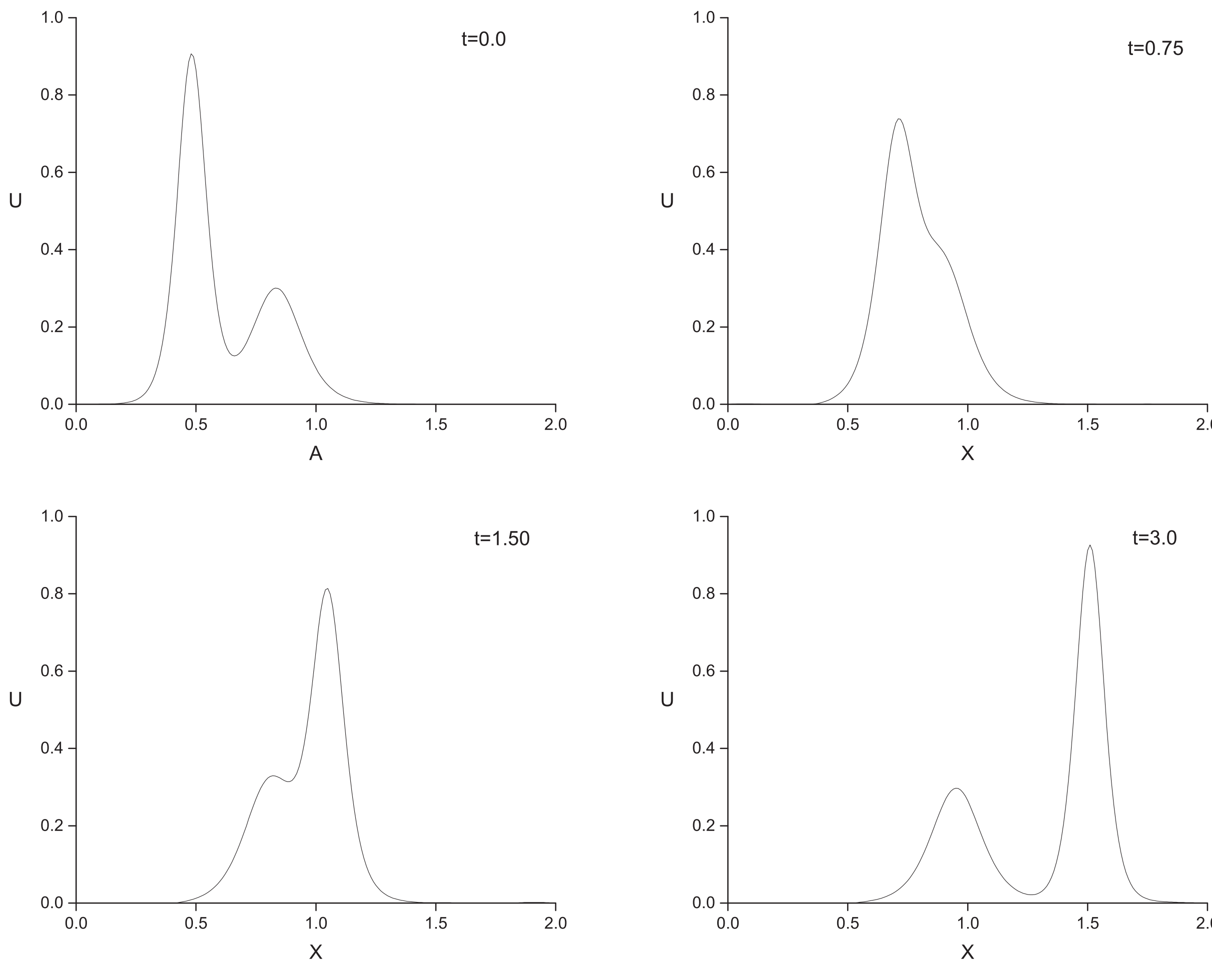

Figure 3. Simulations for double solitons.

4.3. Triple solitons

Our third test problem is reproduction of three solitons from a single solitary wave initial condition is given by [16]

$$U(x,\ 0) = \frac{2}{3}\sec h^2\left(\frac{x - 1}{\sqrt{108\mu}}\right)$$

with values of $\varepsilon = 1,\ \mu = 0.0001,\ \Delta t = 0.0001$, and $N = 751$.

The simulation is run up to time $t = 4$ in the region $[0,\ 3]$. Reproduction of triple waves from single solitary waves is shown in Figure 4. The three lowest invariants are computed and reported with comparison of some earlier works given in Table 6. Relative changes in invariants are also added to Table 6. It is seen noticeably from Table 6 that maximum absolute values of relative changes in invariants are less than 7.3×10^{-7}, 2.6×10^{-6}, and 9.9×10^{-6}, respectively, during the simulation and therefore they can be considered almost constant again.

Table 5. Invariants for double solitons: $\Delta t = 0.0005$ and $N = 201$.

Method	time	I_1	I_2	I_3	$\widehat{I}_1$	$\widehat{I}_2$	$\widehat{I}_3$
Present	0.00	0.228082	0.107062	0.053317	-	-	-
	0.75	0.228078	0.107062	0.053316	-1.4 $\times 10^{-5}$	-4.6 $\times 10^{-6}$	-2.1 $\times 10^{-5}$
	1.50	0.228076	0.107062	0.053316	-2.5 $\times 10^{-5}$	-1.8 $\times 10^{-6}$	-1.4 $\times 10^{-5}$
	3.00	0.228081	0.107063	0.053317	-8.7 $\times 10^{-7}$	5.6 $\times 10^{-6}$	3.0 $\times 10^{-6}$
MQ [15]	0.00	0.228080	0.107061	0.053318			
	0.75	0.228016	0.107055	0.053524			
	1.50	0.228032	0.107057	0.053453			
	3.00	0.227968	0.107061	0.053265			
G [15]	0.00	0.228081	0.107062	0.053316			
	0.75	0.228135	0.107058	0.053312			
	1.50	0.228065	0.107059	0.053313			
	3.00	0.227734	0.107061	0.053316			
IMQ [15]	0.00	0.228081	0.107062	0.053316			
	0.75	0.228964	0.107068	0.053307			
	1.50	0.228917	0.107072	0.053308			
	3.00	0.227399	0.107087	0.053307			
IQ [15]	0.00	0.228081	0.107062	0.053316			
	0.75	0.228456	0.107060	0.053312			
	1.50	0.228386	0.107063	0.053314			
	3.00	0.227576	0.107069	0.053317			
TPS [15]	0.00	0.228079	0.107062	0.053317			
	0.75	0.227689	0.107056	0.053468			
	1.50	0.227633	0.107059	0.053410			
	3.00	0.228071	0.107058	0.053274			

4.4. Maxwellian initial condition

For the fourth test problem we have selected the Maxwellian initial condition given by [18]

$$U(x,\ 0) \ = \ \exp\left(-x^2\right)$$

with boundary conditions $U(-15,\ t) = U(15,\ t) = 0$ to observe propagation of a single solitary wave.

With the value of μ, the solutions will change. The critical value of μ was given as $\mu_c = 0.0625$ in [11]. We have investigated solutions of the Maxwellian initial condition for $\mu = 0.0625$, $\Delta t = 0.001$, and $N = 481$ and we fix the value of $\varepsilon = 1$ to all solutions.

All of the simulations are run up to time $t = 10$ and shown in Figure 5. When the critical value of μ is used in simulations as $\mu_c = 0.0625$ the single solitary wave is observed with no oscillatory tail. This is the result of balance between the nonlinear and dispersive effects [11]. By decreasing the value of μ to $\mu = 0.04$ with

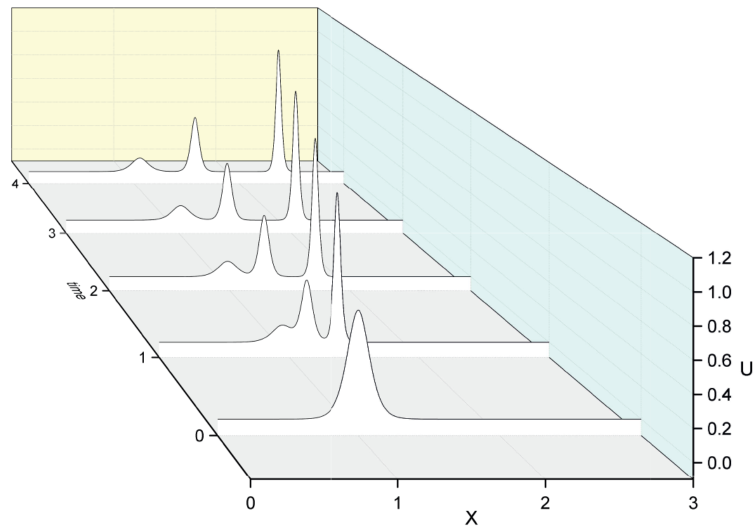

Figure 4. Simulations of triple solitons time up to $t = 3$

Table 6. Invariants for triple solitons: $\Delta t = 0.0001$ and $N = 871$.

	MCBC-DQM (Present)					
t	$I_1 \times 10^1$	$I_2 \times 10^2$	$I_3 \times 10^2$	$\widehat{I}_1$	$\widehat{I}_2$	$\widehat{I}_3$
0	1.38564000	6.15839900	3.14763000	-	-	-
1	1.38564000	6.15841400	3.14766100	0.0×10^{-9}	2.4×10^{-6}	9.8×10^{-6}
2	1.38564100	6.15841500	3.14766000	7.2×10^{-7}	2.5×10^{-6}	9.5×10^{-6}
3	1.38564100	6.15841200	3.14766000	7.2×10^{-7}	2.1×10^{-6}	9.5×10^{-6}
4	1.38564000	6.15840800	3.14765600	0.0×10^{-9}	1.4×10^{-6}	8.2×10^{-6}
t	CDQ [22]			LPDQ [22]		
0	1.38564063	6.15840287	3.14762813	1.38564063	6.15840287	3.14762811
1	1.38565309	6.15844240	3.14760463	1.38543443	6.15842579	3.14756106
2	1.38563108	6.15857397	3.14774386	1.38531080	6.15865591	3.14754356
3	1.38563254	6.15866382	3.14788540	1.38537991	6.15896863	3.14745087
4	1.38562387	6.15885831	3.14802419	1.38564064	6.15923613	3.14714932

$\Delta t = 0.001$ and $N = 551$ we observe a solitary wave with an oscillatory tail behind of the wave (Figure 5). By the decreasing of value of μ to $\mu = 0.01$ with $\Delta t = 0.001$ and $N = 661$ we observe three solitary waves and for the lowest value of $\mu = 0.001$ with $\Delta t = 0.001$ and $N = 1201$ we observe nine solitons (Figure 5). The three lowest invariants are computed and reported as given in Table 7. Relative changes in invariants are also added to Table 7. It is seen noticeably from Table 7 that the maximum absolute values of relative changes in invariants for the values of μ from $\mu = 0.0625$ to $\mu = 0.001$ are less than 8.0×10^{-4}, 1.6×10^{-4}, 7.9×10^{-5}, and 8.3×10^{-4}, respectively, during all simulations and therefore they can be considered almost constant again.

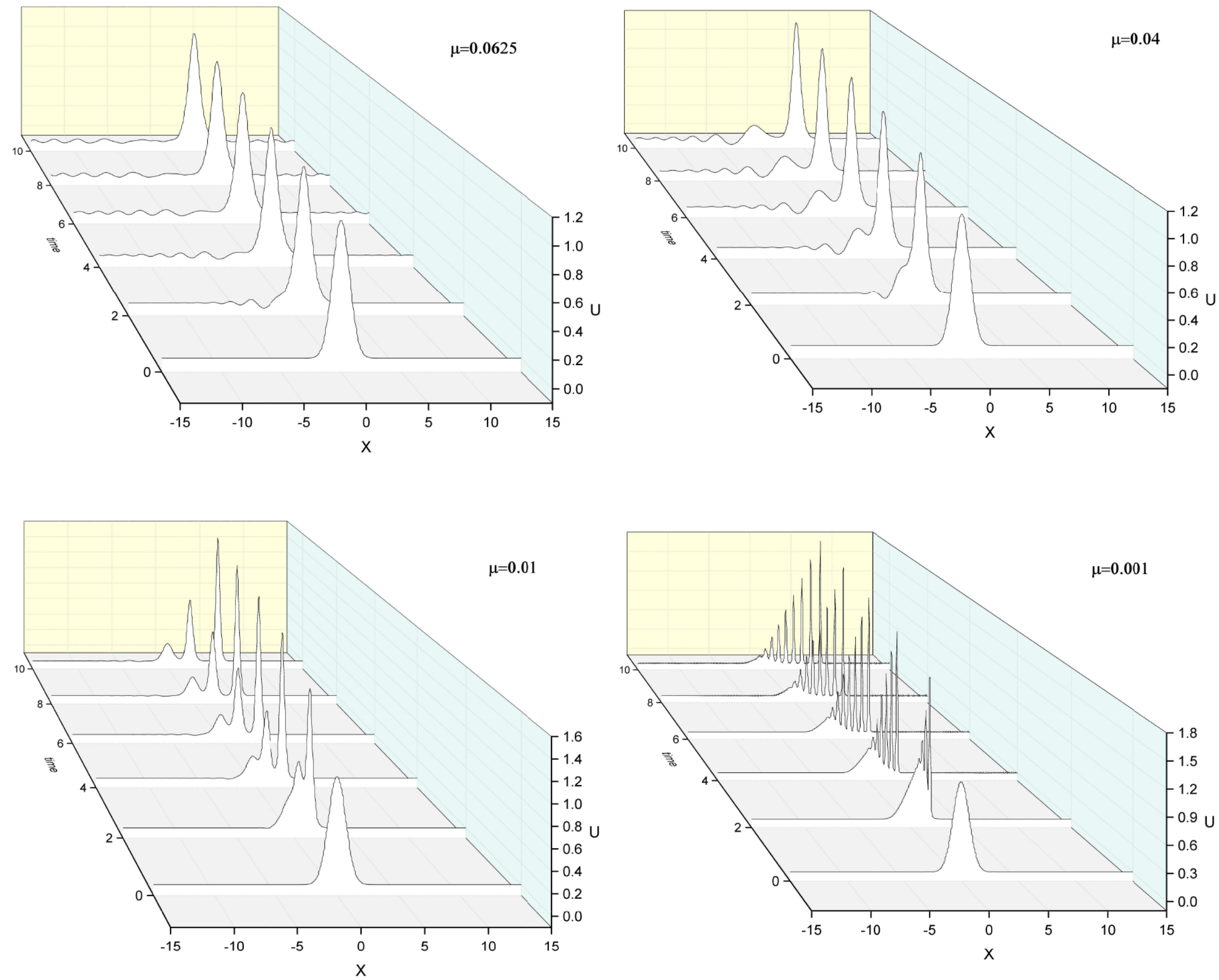

Figure 5. Simulations for Maxwellian initial condition.

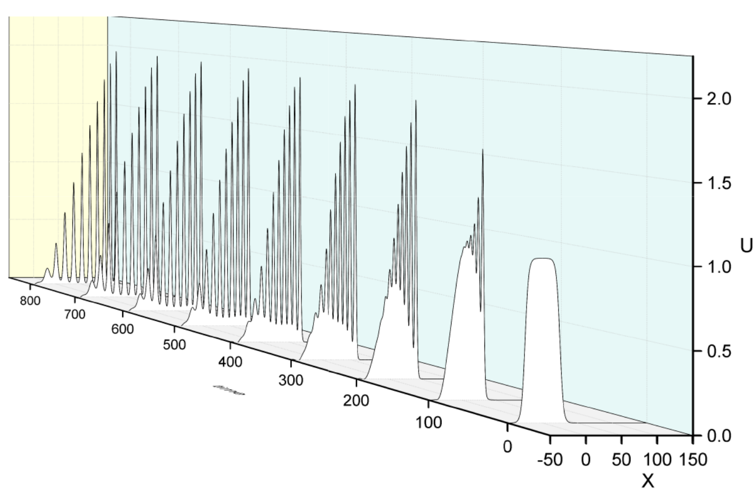

Figure 6. Simulations of train of ten solitons time up to t = 800.

Table 7. Invariants for Maxwellian initial condition.

μ	Time	I_1	I_2	$I_3 \times 10^1$	$\widehat{I}_1$	$\widehat{I}_2$	$\widehat{I}_3$
0.0625	0	1.772454	1.253314	7.883310	-	-	-
	2	1.772455	1.253314	7.883322	5.6×10^{-7}	0.0×10^{-9}	1.5×10^{-6}
	4	1.772972	1.253310	7.883376	2.9×10^{-4}	-3.1×10^{-6}	8.3×10^{-6}
	6	1.772925	1.253329	7.883488	2.6×10^{-4}	1.1×10^{-5}	2.2×10^{-5}
	8	1.773667	1.253245	7.883575	6.8×10^{-4}	-5.5×10^{-5}	3.3×10^{-5}
	10	1.771050	1.253196	7.883694	-7.9×10^{-4}	-9.4×10^{-5}	4.8×10^{-5}
0.04	0	1.772454	1.253314	8.729294	-	-	-
	2	1.772460	1.253315	8.729322	3.3×10^{-6}	7.9×10^{-7}	3.2×10^{-6}
	4	1.772377	1.253314	8.729339	-4.3×10^{-5}	0.0×10^{-9}	5.1×10^{-6}
	6	1.772443	1.253315	8.729348	-6.2×10^{-6}	7.9×10^{-7}	6.1×10^{-6}
	8	1.772185	1.253315	8.729380	-1.5×10^{-4}	7.9×10^{-7}	9.8×10^{-6}
	10	1.772307	1.253325	8.729328	-8.2×10^{-5}	8.7×10^{-6}	3.8×10^{-6}
0.01	0	1.772453	1.253314	9.857275	-	-	-
	2	1.772453	1.253323	9.857627	0.0×10^{-9}	7.1×10^{-6}	3.5×10^{-5}
	4	1.772453	1.253331	9.857994	0.0×10^{-9}	1.3×10^{-5}	7.2×10^{-5}
	6	1.772451	1.253332	9.858038	-1.1×10^{-6}	1.4×10^{-5}	7.7×10^{-5}
	8	1.772451	1.253332	9.858042	-1.1×10^{-6}	1.4×10^{-5}	7.7×10^{-5}
	10	1.772443	1.253332	9.858044	-5.6×10^{-6}	1.4×10^{-5}	7.8×10^{-5}
		I_1	I_2	I_3			
0.001	0	1.772454	1.253314	1.019567	-	-	-
	2	1.772452	1.253399	1.019973	-1.1×10^{-6}	6.7×10^{-5}	3.9×10^{-4}
	4	1.772437	1.253493	1.020409	-9.5×10^{-6}	1.4×10^{-4}	8.2×10^{-4}
	6	1.772429	1.253503	1.020408	-1.4×10^{-5}	1.5×10^{-4}	8.2×10^{-4}
	8	1.772435	1.253510	1.020383	-1.0×10^{-5}	1.5×10^{-4}	8.0×10^{-4}
	10	1.772494	1.253513	1.020388	2.2×10^{-5}	1.5×10^{-4}	8.0×10^{-4}

4.5. Train of solitons

Our fifth and the last test problem has the initial condition given by [19]

$$U(x,\ 0)\ =\ 0.5\left[1\ -\ \tanh\frac{|x|\ -\ x_0}{d}\right], \tag{26}$$

and boundary conditions

$$U(-50,\ t)\ =\ U(150,\ t)\ =\ 0, \tag{27}$$

where $-50\ \leq\ x\ \leq\ 150$, $d\ =\ 5$, and $x_0\ =\ 25$ will be considered in all simulations.

The solution vector after a very long run time $t\ =\ 800$ with $\varepsilon\ =\ 0.2$, $\mu\ =\ 0.1$, $\Delta t\ =\ 0.02$, and $\Delta x\ =\ 0.2$ has been shown in Figure 6. A train of 10 solitons has been formed at the end of the simulation. The invariants I_1, I_2, and I_3 are recorded and reported with relative changes in invariants in Table 8 for the present case. It is noticeably seen from Table 8 that the maximum absolute values of relative changes in invariants are less than $9.2\ \times\ 10^{-6}$, $4.5\ \times\ 10^{-6}$, and $1.8\ \times\ 10^{-5}$, respectively, during this very long run and therefore they can be considered almost constant.

Table 8. Invariants for train of solitons: $\Delta t = 0.02$ and $\Delta x = 0.2$.

	MCBC-DQM (Present)						CDQ [22]		
t	I_1	I_2	I_3	$\widehat{I}_1$	$\widehat{I}_2$	$\widehat{I}_3$	I_1	I_2	I_3
0	50.00011	45.00043	42.30065	-	-	-	50.00010	45.00045	42.30068
200	50.00042	45.00053	42.30111	6.1×10^{-6}	2.2×10^{-6}	1.0×10^{-5}	49.99671	45.00095	42.30104
400	49.99988	45.00053	42.30135	-4.5×10^{-6}	2.2×10^{-6}	1.6×10^{-5}	50.01744	45.00457	42.30368
600	49.99966	45.00063	42.30138	-8.9×10^{-6}	4.4×10^{-6}	1.7×10^{-5}	50.00556	45.00313	42.30273
800	50.00057	45.00059	42.30137	9.1×10^{-6}	3.5×10^{-6}	1.7×10^{-5}	49.94377	45.01907	42.31425
t	FEM [4]			FEM [40]			FEM [41]		
0	50.00	45.000	42.301	50.00021	45.00055	42.30074	50.00000	45.00041	42.30065
200	50.01	45.014	42.110	50.00058	44.99962	42.30098	49.99166	45.00441	42.30647
400	50.00	45.028	42.033	50.00237	44.99921	42.30135	50.06452	45.00995	42.31197
600	49.98	45.042	42.049	49.97857	44.99820	42.29995	50.15105	45.01577	42.31489
800	50.02	45.056	42.064	49.96331	44.99803	42.29974	49.97169	45.02899	42.32111

4.6. Stability analysis

A matrix stability analysis is also investigated for the MCBC-DQM. We have used MATLAB to obtain the eigenvalues of the coefficient matrix for all of the test problems. Eigenvalues of the suggested method for $N = 201$, $N = 301$, $N = 401$, and $N = 501$ number of grids are presented in Figure $7-11$. The maximum absolute values of eigenvalues for all of the test problems at various numbers of grid points are also tabulated in Table 9. The eigenvalues have real and imaginary parts for all numbers of grid points. As the numbers of grid points increase, eigenvalues get greater. This means that to get into the stability region time increments must be decreased. All the eigenvalues are consistent with the stability criteria [21].

Table 9. Maximum absolute value of eigenvalues at various numbers of grid points.

	Grid Number	201	301	401	501
Single	Max$\lvert Re(\lambda) \rvert$	5.0620×10^3	1.7084×10^4	4.0496×10^4	7.9094×10^4
	Max$\lvert Im(\lambda) \rvert$	1.5462×10^4	5.2275×10^4	1.2399×10^5	2.4223×10^5
Double	Max$\lvert Re(\lambda) \rvert$	5.0620×10^3	1.7084×10^4	4.0441×10^4	7.9025×10^4
	Max$\lvert Im(\lambda) \rvert$	1.5454×10^4	5.2262×10^4	1.2397×10^5	2.4220×10^5
Triple	Max$\lvert Re(\lambda) \rvert$	1.0459×10^3	3.5298×10^3	4.0496×10^4	7.9094×10^4
	Max$\lvert Im(\lambda) \rvert$	3.2013×10^3	1.0810×10^4	8.3670×10^3	1.6342×10^4
Maxw.	Max$\lvert Re(\lambda) \rvert$	6.5367×10^5	2.2061×10^6	5.2294×10^6	1.0214×10^7
	Max$\lvert Im(\lambda) \rvert$	2.0014×10^6	6.7575×10^6	1.6020×10^7	3.1291×10^7
Train	Max$\lvert Re(\lambda) \rvert$	1.0459×10^6	3.5298×10^6	8.3670×10^6	1.6342×10^7
	Max$\lvert Im(\lambda) \rvert$	3.2023×10^6	1.0812×10^7	2.5632×10^7	5.0065×10^7

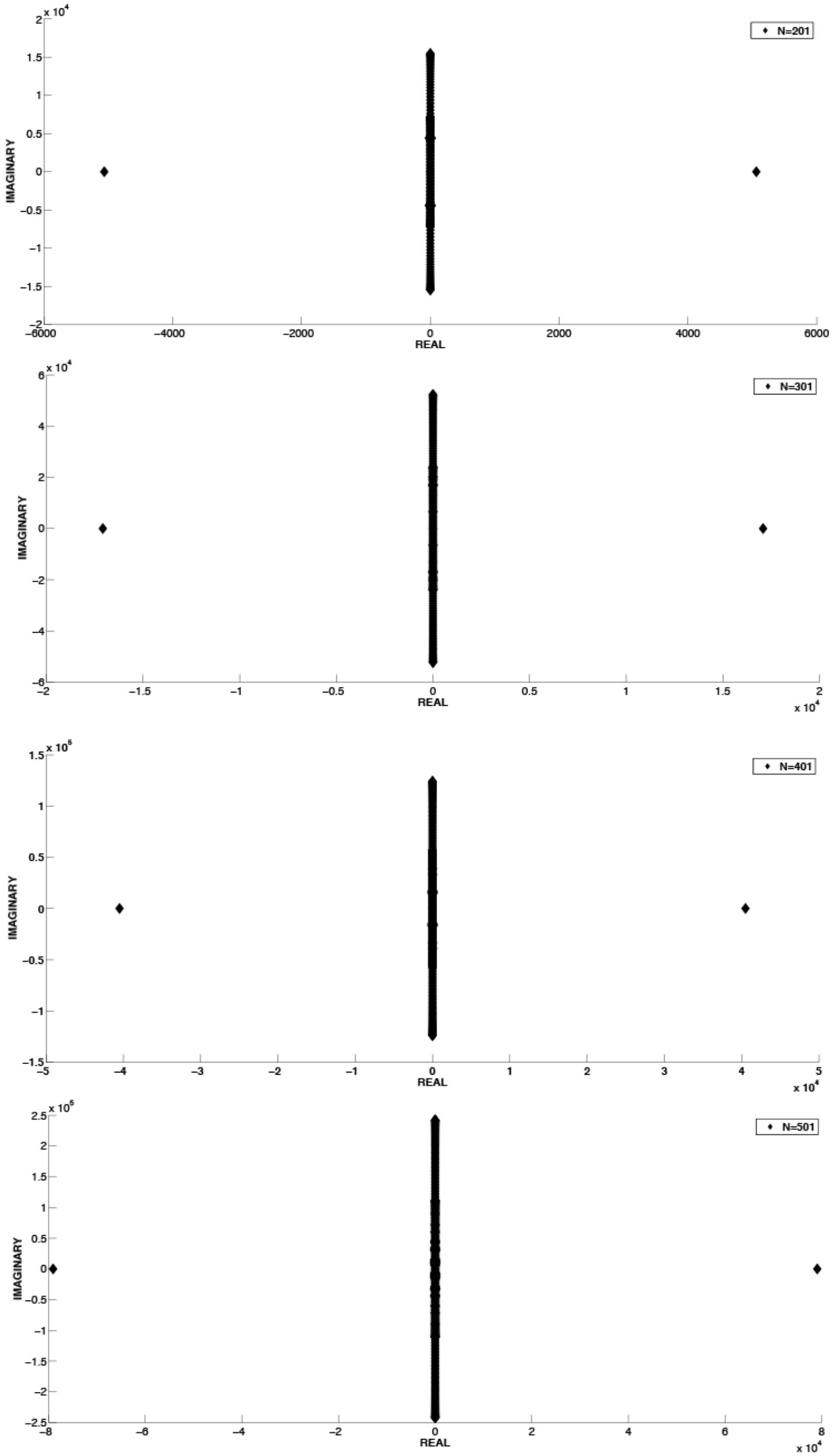

Figure 7. Eigenvalues for single soliton.

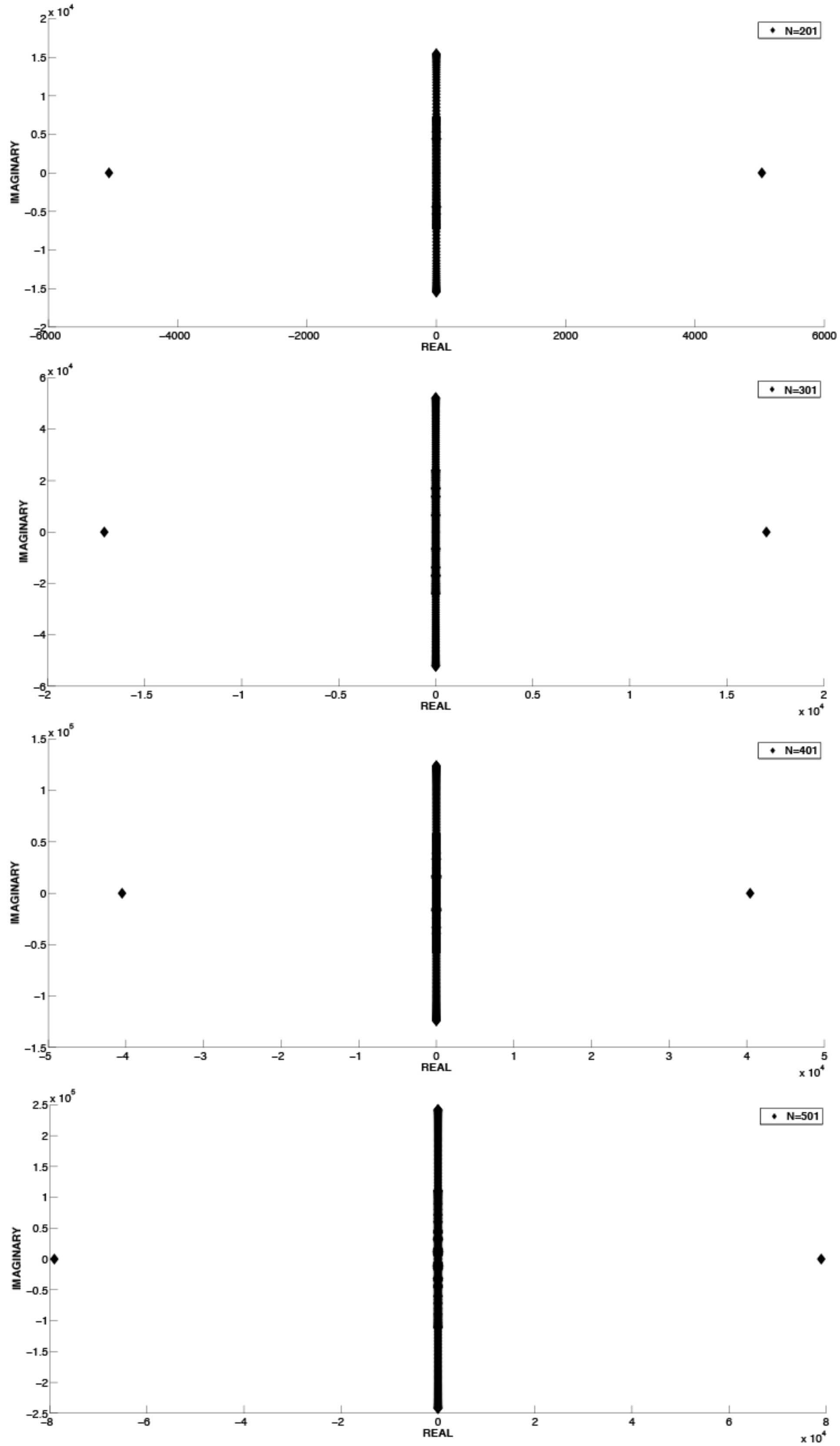

Figure 8. Eigenvalues for double solitons.

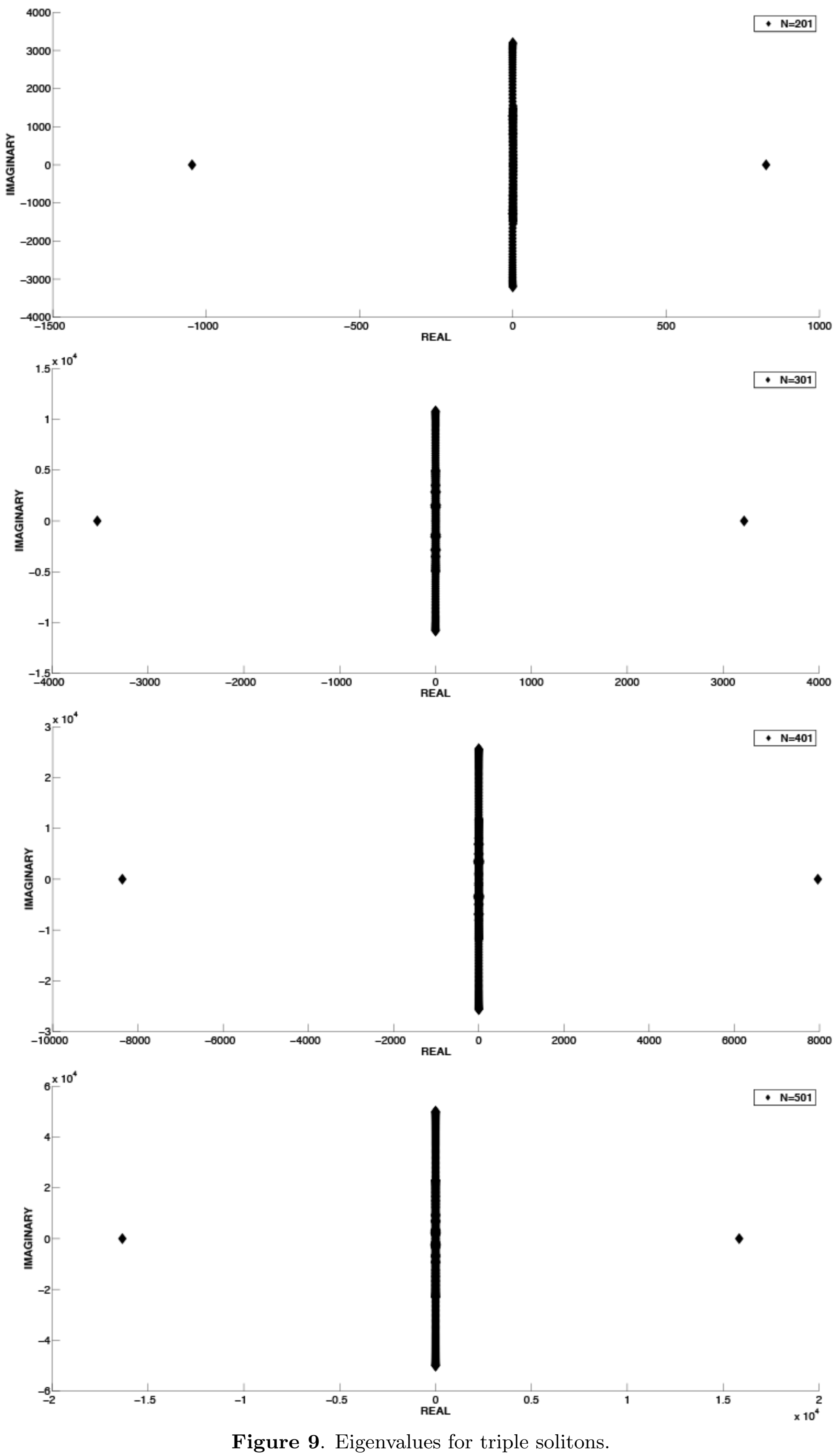

Figure 9. Eigenvalues for triple solitons.

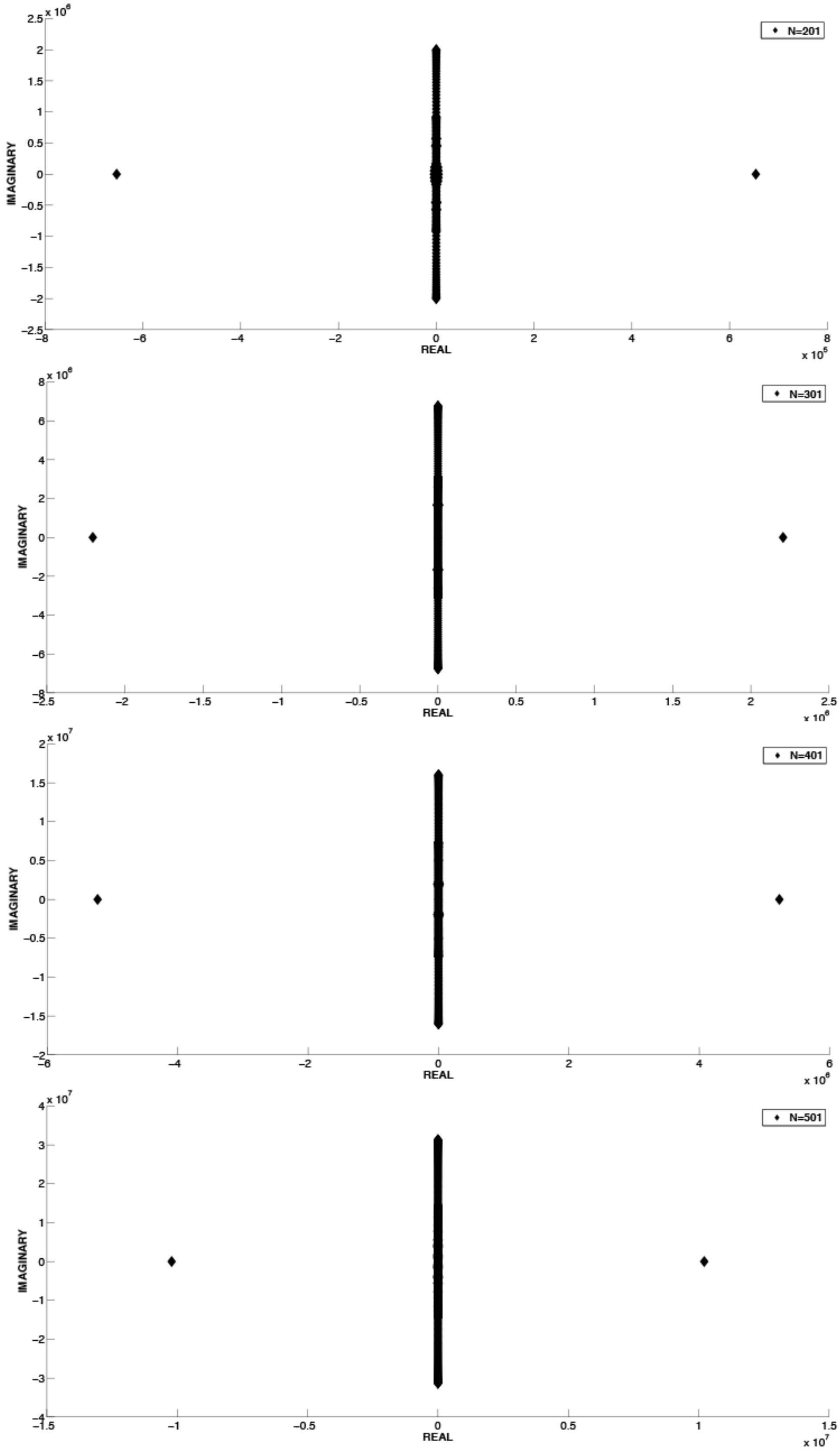

Figure 10. Eigenvalues for Maxwellian initial condition.

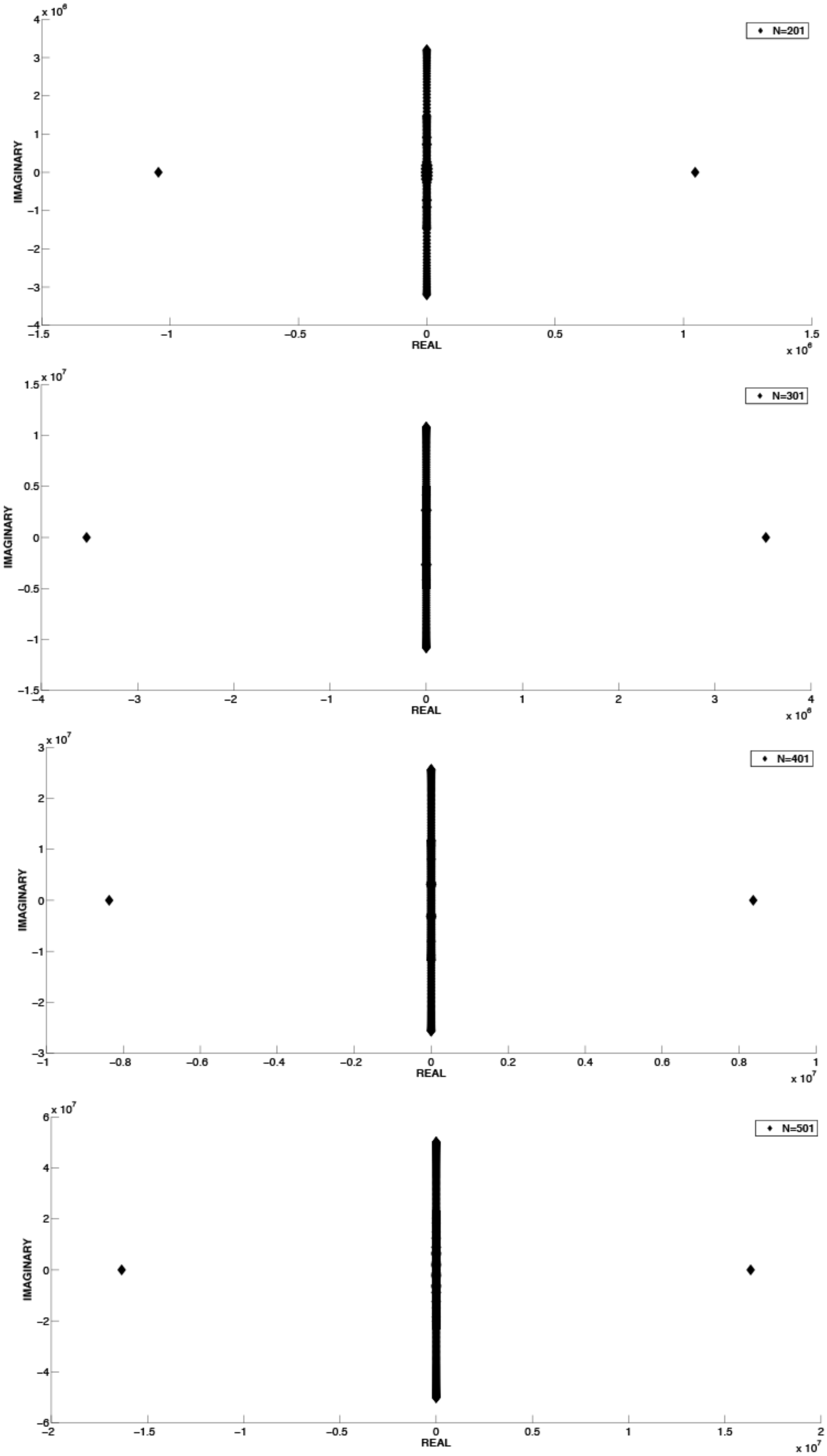

Figure 11. Eigenvalues for train of solitons.

5. Conclusion

In this work, we have implemented DQM based on modified cubic B-splines for numerical approximation of KdV equation. Five different test problems have been solved. The performance and accuracy of the present method have been shown by calculating and comparing the L_2 and L_∞ error norms with earlier works. As it seen at Table 2, the present results are acceptable good when compared with some earlier works. As it seen at Table 3, the present results are better than cubic-DQM[22]. Three lowest invariants are calculated and reported for all of the test problems. The obtained invariants are acceptable good when compared with some earlier works. Stability analysis have been done for all of the test problems and all of the eigenvalues are in convenience with stability criteria [21]. So, MCBC-DQM may be useful to get the numerical solutions of other important nonlinear problems.

References

[1] Ablowitz MJ, Clarkson PA. Solitons, Nonlinear Evolution Equations and Inverse Scattering. New York, NY, USA: Cambridge, 1991.

[2] Ablowitz MJ, Segur H. Solitons and Inverse Scattering Transform. Philadelphia, PA, USA: Siam, 1981.

[3] Alexander ME, Morris JL. Galerkin methods for some models equations for nonlinear dispersive waves. J Comput Phys 1979; 30: 428-451.

[4] Ali AHA, Gardner LRT, Gardner GA. Numerical study of the KdVB equation using B-spline finite elements. J Math Phys Sci 1993; 27: 37-53.

[5] Başhan A. Numerical solutions of some partial differential equations with B-spline differential quadrature method. PhD, İnönü University, Malatya, Turkey, 2015.

[6] Başhan A, Karakoç SBG, Geyikli T. Approximation of the KdVB equation by the quintic B-spline differential quadrature method. Kuwait J Sci 2015; 42: 67-92.

[7] Başhan A, Karakoç SBG, Geyikli T. B-spline Differential Quadrature Method for the Modified Burgers' Equation. CUJSE 2015; 12: 001-013.

[8] Başhan A, Uçar Y, Yağmurlu NM, Esen A. Numerical solution of the complex modified Korteweg-de Vries equation by DQM. Journal of Physics: Conference Series 2016; doi:10.1088/1742-6596/766/1/012028.

[9] Bellman R. Differential quadrature: a technique for the rapid solution of nonlinear differential equations. Journal of Computational Physics 1972; 40-52.

[10] Bellman R, Kashef B, Lee ES, Vasudevan R. Differential Quadrature and Splines. Computers and Mathematics with Applications 1976; 371-376.

[11] Berezin YuA, Karpman VA. Nonlinear evolution of disturbances in plasmas and other dispersive media. Sov Phys JETP 1967; 24: 1049-1056.

[12] Bonzani I. Solution of non-linear evolution problems by parallelized collocation-interpolation methods. Computers & Mathematics and Applications 1997; 34: 71-79.

[13] Bullough R, Caudrey P. Solitons vol 17 in "Topics in Current Physics". Berlin, Germany: Springer, 1980.

[14] Cheng J, Wang B, Du S. A theoretical analysis of piezoelectric/composite laminate with larger-amplitude deflection effect, Part II: hermite differential quadrature method and application. International Journal of Solids and Structures 2005; 42: 6181-6201.

[15] Dağ I, Dereli Y. Numerical solutions of KdV equation using radial basis functions. Appl Math Model 2008; 32: 535-546.

[16] Debussche A, Printems J. Numerical simulation of the stochastic Korteweg-de Vries equation. Physica D 1999; 134: 200-226.

[17] Drazin PG, Johnson RS. Solitons: an Introduction. New York, NY, USA: Cambridge, 1996.

[18] Gardner GA, Ali AHA, Gardner LRT. Simulations of solitons using quadratic spline shape functions. UCNW Maths 1989; 89.03.

[19] Gardner LRT, Gardner GA, Ali AHA. A finite element solution for the Korteweg-de Vries equation using cubic B-splines. UCNW Maths 1989; 89.01.

[20] Karakoç SBG, Başhan A, Geyikli T. Two different methods for numerical solution of the modified Burgers' equation. The Scientific World Journal 2014; http://dx.doi.org/10.1155/2014/780269.

[21] Ketcheson DI. Highly efficient strong stability preserving Runge-Kutta methods with low-storage implementations. Siam J Sci Comput 2008; 30: 2113-2136.

[22] Korkmaz A. Numerical solutions of some one dimensional partial differential equations using B-spline differential quadrature methods. PhD, Eskişehir Osmangazi University, Eskişehir, Turkey, 2010.

[23] Korkmaz A. Numerical algorithms for solutions of Korteweg-de Vries equation. Numer Methods Partial Differential Eq 2010; 26: 1504-1521.

[24] Korkmaz A, Dağ I. Shock wave simulations using Sinc Differential Quadrature Method. International Journal for Computer-Aided Engineering and Software 2011; 28: 654-674.

[25] Korkmaz A, Dağ I. Cubic B-spline differential quadrature methods for the advection-diffusion equation. International Journal of Numerical Methods for Heat & Fluid Flow 2012; 22: 1021-1036.

[26] Korkmaz A, Dağ I. Numerical simulations of boundary-forced RLW equation with cubic B-spline-based differential quadrature methods. Arab J Sci Eng 2013; 38: 1151-1160.

[27] Mittal RC, Jain RK. Numerical solutions of nonlinear Burgers' equation with modified cubic B-splines collocation method. Appl Math Comp 2012; 218: 7839-7855.

[28] Prenter PM. Splines and Variational Methods. New York, NY, USA: John Wiley & Sons, 1975.

[29] Quan JR, Chang CT. New sightings in involving distributed system equations by the quadrature methods-I. Comput Chem Eng 1989; 13: 779-788.

[30] Quan JR, Chang CT. New sightings in involving distributed system equations by the quadrature methods-II. Comput Chem Eng 1989; 13: 1017-1024.

[31] Sanz Serna JM, Christie I. Petrov-Galerkin methods for nonlinear dispersive waves. J Comput Phys 1981; 39: 94-102.

[32] Shu C, Wu YL. Integrated radial basis functions-based differential quadrature method and its performance. Int J Numer Meth Fluids 2007; 53: 969-984.

[33] Shu C. Differential Quadrature and Its Application in Engineering. London, UK: Springer-Verlag, 2000.

[34] Soliman AA. Collocation solution of the Korteweg-de Vries equation using septic splines. Int J Comput Maths 2004; 81: 325-331.

[35] Soliman AA, Ali AHA, Raslan KR. Numerical solution for the KdV equation based on similarity reductions. Applied Mathematical Modelling 2009; 33: 1107-1115.

[36] Spiteri JR, Ruuth SJ. A new class of optimal high-order strong stability-preserving time-stepping schemes. Siam J Numer Anal 2002; 40: 469-491.

[37] Striz AG, Wang X, Bert CW. Harmonic differential quadrature method and applications to analysis of structural components. Acta Mechanica 1995; 111: 85-94.

[38] Taha TR, Ablowitz MJ. Analytical and numerical aspects of certain nonlinear evolution equations III. Numerical, Korteweg-de Vries equation. J Comput Phys 1984; 55: 231-253.

[39] Zabusky NJ. A synergetic approach to problem of nonlinear dispersive wave propagation and interaction. Ames W, editor. Proceedings Symposium on nonlinear partial differential equations. Academic Press, New York, NY, USA, 1967; pp. 223-258.

[40] Zaki SI. A quintic B-spline finite elements scheme for the KdVB equation. Comput Meth Appl Mech Engrg 2000; 188: 121-134.

[41] Zaki SI. Solitary waves of the Korteweg-de Vries-Burgers' equation. Comput Phys Commun 2000; 126: 207-218.